Applied Catalysis B: Environmental 84 (2008) 233–240

Contents lists available at ScienceDirect

Applied Catalysis B: Environmental

journal homepage: www.elsevier.com/locate/apcatb

Photodegradation of dye pollutant under UV light by nano-catalyst doped titania thin films

Sunil Dutta Sharma *, K.K. Saini, Chander Kant, C.P. Sharma, S.C. Jain

Liquid Crystal & Self Assembled Monolayer Section, National Physical Laboratory, New Delhi 110012, India

ARTICLE INFO

Article history:
Received 16 November 2006
Received in revised form 28 March 2008
Accepted 5 April 2008
Available online 22 April 2008

Keywords:
Mn-doped TiO_2 films
Sol–gel
Photodegradation
Methylene blue

ABSTRACT

Undoped and manganese ion-doped TiO_2 powders and thin films have been prepared by sol–gel route. The concentration of the manganese in TiO_2 powders and films varied from 2 to 10 mol%. These powders were annealed at different temperatures from 300 to 1000 °C while films were annealed at 450 °C for 1 h. Prepared samples were characterized by XRD, SEM, XPS, spectroscopic and contact angle measurement techniques.

Photocatalytic activity, in terms of rate constant measured by degradation of methylene blue dye, under UV exposure was found to increase from 0.27 to 0.36 for 5 mol% doping while very small photo activity has been observed under visible light exposure. Hydrophillicity also shows the same behavior. Optical studies revealed the generation of allowed energy band in the forbidden gap at ~0.63 eV below the conduction band. It has been concluded that Mn doping increases photocatalytic activity by scavenging the photogenerated electrons, thereby increasing the life time of charge carriers and increasing the exposed surface area by reducing the crystallite size.

1. Introduction

Heterogeneous photocatalysis has been the subject of numerous investigations as it is an attractive technique for the complete destruction of undesirable contaminants (pollutants) in both the liquid and gaseous phase by using solar or artificial light illumination. Titania photocatalysis advantages, such as low operation temperature, low cost, low energy consumption, have led the relevant applications to the stage of commercialization. Recently, considerable research is focused on TiO_2 composites and thin films to improve the photocatalytic activity and shift the fundamental absorption edge towards longer wavelengths [1–4].

TiO_2 crystallizes in three polymorphic forms: anatase (tetragonal), rutile (tetragonal) and brookite (orthorhombic). Out of two stable phases, anatase and rutile, only anatase phase is found suitable for photocatalytic degradation of organic pollutants in water and air. This property of the anatase phase has been assigned due to the position of Fermi level and nature of forbidden band gap [5–7]. Due to large band gap of anatase TiO_2 ~3.2 eV, the photon absorption, for electronic excitation, is limited only to the UV range and hence exhibits limited photoactivity in the solar exposure. Number of research reports has appeared to change photocatalytic properties of this by different procedures. Some researchers have studied the photocatalytic properties under different preparation conditions [8,9] while others have reported the photoactivity with different dopants like Mn^{2+}, Cr^{3+}, Co^{2+}, Fe^{3+} [10,11]. Decrease in photocatalytic activity has been reported by Palmisano et al. [12] by doping the sample with Cr^{3+} and increase in photoactivity has been reported by Gracien et al. and Wang et al. [13,14] with dopants Mn^{2+} and Fe^{3+}. The role of dopant, on controlling the photoactivity, has not been established clearly. We have studied the effect of Mn doping on the photocatalytic properties of TiO_2 and explained our observations in the light of microstructure and energy band positions of the material.

2. Experimental

2.1. Preparation of the sol, films and powder

The sol for coating the film, was prepared from titanium tetrabutoxide, $Ti(OC_4H_9)_4$ in isopropyl alcohol ($CH_3CHOHCH_3$) as solvent. Calculated quantity of water (H_2O) was added to it for the hydrolysis and polycondensation reaction in presence of nitric acid (HNO_3) as a catalyst. The composition of undoped TiO_2 sol was $Ti(OC_4H_9)_4/CH_3CHOHCH_3/H_2O/HNO_3$ – 1:26:2:0.2 in molar ratio. Concentration of Mn ions, in the sol, was varied between 2 and 10 mol% by adding calculated amount of manganese acetylacetonate [$Mn(CH_3COCHCOCH_3)_2$] to it. The obtained sol was acidic in

* Corresponding author. Tel.: +91 11 45609486.
E-mail address: sunil_vans@mail.nplindia.ernet.in (S.D. Sharma).

0926-3373/$ – see front matter © 2008 Elsevier B.V. All rights reserved.
doi:10.1016/j.apcatb.2008.04.017

nature (pH ~ 2–3) which was kept overnight for 24 h at 25 °C temperature before coating. Doped and undoped TiO_2 films were fabricated on the ultrasonically cleaned glass substrate by the dip coating process at a withdrawal speed of 12 cm/min. Films of different thickness were obtained by multiple coatings with intermediate drying between the successive coatings at 150 °C for 30 min. Dried films were finally annealed at 450 °C for 1 h. For the structural studies, the corresponding gels were allowed to dry naturally for about 20 days, followed by drying in an oven at 150 °C for 30 min. These powders were finally annealed at different temperatures from 300 to 1000 °C for 1 h.

2.2. Characterizations of the films and powder

To identify the crystal phase of the annealed samples, XRD spectra was recorded for 2θ range from 20° to 80° with SIEMENS D-500 diffractometer using monochromatized CuKα radiation (λ = 1.541 A°). Surface morphology and film thickness measurements were carried out using LEO-440 Scanning Electron Microscope (SEM). X-ray photoelectron spectroscopy (XPS) studies were carried out on a PerkinElmer ϕ model with hemispherical XPS analyzer using AlKα radiations. All the spectra, presented here are corrected by taking carbon peak at a standard value of 286.4 eV. Transmittance and absorption spectra were recorded from 300 to 800 nm range with SHIMADZU UV-3101 PC UV-VIS spectrophotometer at normal incidence. Photoluminescence spectra were recorded with PerkinElmer LS55 spectrophotometer. The hydrophillicity of the films was studied in terms of contact angle measurement by a sessile drop method using (KRUSS DSA 10 MK2) a CCD camera.

2.3. Photocatalytic measurements

TiO_2 films are settled in aqueous methylene blue with a concentration of 10 mg/l in a quartz cell (10 mm × 10 mm × 30 mm). A high-pressure mercury lamp (125 W) is used as UV light source and an electric bulb (100 W) is used as source of visible light. The averaged intensity of UV irradiance, measured with a UV irradiance meter (Model UV-A), is 0.5 mW cm^{-2} in the wavelength range 320–400 nm with peak position at 365 nm. One face (10 mm × 30 mm) of the cell is irradiated with desired photons so as the incident light falls normally on the coated substrate surface. Air is bubbled through the solution, during irradiation, to eliminate the diffusion gradient related errors. Photocatalytic activity is estimated by measuring the residual concentration of methylene blue in the solution. The concentration of methylene blue, in aqueous solution is calculated by measuring the absorbance (peak intensity) of the solution at 664 nm with UV-visible spectrophotometer and using the empirical relation:

$$A = 0.0725C$$

3. Results and discussion

3.1. Structural studies

Typical XRD patterns of undoped TiO_2 powder annealed at 450 and 800 °C and 8 mol% Mn-doped TiO_2 powders annealed at 600 °C for 1 h are shown in Fig. 1. Diffraction peaks corresponding to anatase and rutile phases have been marked with 'A' and 'R', respectively, along with the corresponding diffraction planes. No rutile phase formation has been observed in pure TiO_2 samples annealed below 800 °C whereas in case of Mn^{2+} doped samples peaks corresponding to rutile and anatase phases have been observed in samples annealed at 600 °C. It is evident, from these studies, that Mn doping reduces the phase transformation temperature from anatase to rutile. The decrease in the phase transition temperature with Mn^{2+} doping is attributed to the oxygen vacancies in the structure caused by doping; essential for charge compensation of lower valent cations. These vacancies enhance the transport of atoms required for phase transition from anatase to rutile [15]. This is exactly the reverse phenomenon reported in the doping of higher valent cations, where phase transition has been expected to be retarded by forming interstitial Ti^{3+} cations that suppresses atomic transport in the anatase phase [16]. Therefore, the effect of Mn doping is to introduce oxygen vacancies in the TiO_2 structure which enhances the diffusion of atoms in the system. This mechanism is supposed to be responsible for the phase transition of Mn-doped TiO_2 at lower temperatures as compared to undoped samples.

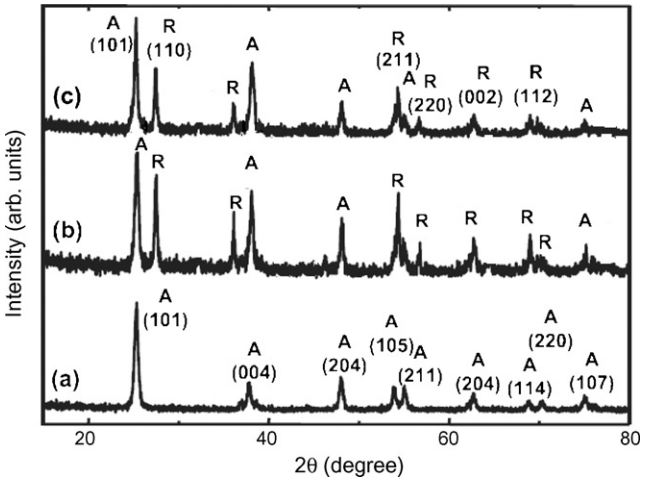

Fig. 1. XRD spectra of (a) pure TiO_2 powder annealed at 450 °C, (b) pure TiO_2 powder annealed at 800 °C and (c) 8 mol% manganese doped TiO_2 powder annealed at 600 °C for 1 h.

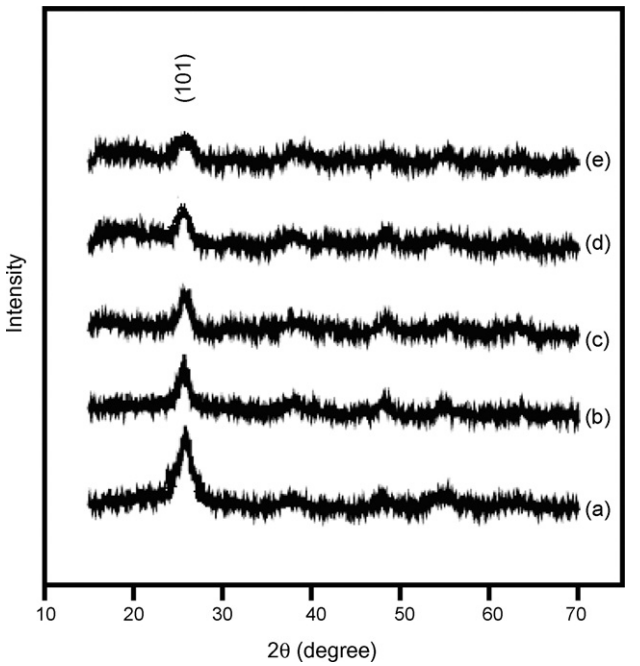

Fig. 2. XRD spectra of (a) pure TiO_2 film, (b) 2 mol%, (c) 5 mol%, (d) 8 mol% and (e) 10 mol% manganese doped TiO_2 film on soda glass annealed at 450 °C for 1 h.

We have calculated the grain size of TiO_2 particles in the film by Scherrer's method [17] from the peak corresponding to (1 0 1) plane of anatase phase (25.8°) Fig. 2. The crystallite size in undoped films is ~30 nm. As doping level in TiO_2 is increased, the FWHM of 101 peak increases, this clearly indicates that doped samples have smaller grain size.

We have not observed characteristic peaks of manganese oxides in the XRD patterns even if the dopant level in the solution is as high as 10 mol%. This implies either manganese was incorporated in the crystallite of TiO_2 or manganese oxide was very small and highly dispersed [18].

Similar properties have been shown by pure and 2–10 mol% Mn-doped TiO_2 films on soda glass, annealed at 450 °C for 1 h (Fig. 2). FWHM of 101 peak, which corresponds to anatase phase also increases with increasing the concentration of Mn. No peak, in the XRD patterns, corresponding to manganese oxide (MnO) was observed in Mn-doped films. These observations also support the above findings on powder samples.

Surfaces of undoped and Mn-doped TiO_2 films are quiet smooth, as observed by SEM. The surface morphology of 2 mol% TiO_2 is similar to that of pure TiO_2 film Fig. 3. However, a gradual decrease in crystallite size with increase in doping level is observed for further doping levels. Whole surface of the film shows regular structure, a uniform distribution of voids in all the films has been observed. Increased surface area with decreased particle size is the property of this type of morphology, which provides more exposed area to incident photons/radiations.

3.2. XPS studies

XPS spectra of Ti 2p core levels of pure and Mn-doped TiO_2 film taken at slow scan is shown in Fig. 4. The binding energy peaks corresponding to Ti $2p_{3/2}$ and Ti $2p_{1/2}$ lines for pure TiO_2 films are observed at 458.4 and 464.1 eV, which have peak separation of 5.7 eV, indicating the presence of Ti^{4+} (TiO_2) in these films [19]. The binding energy peaks of Ti $2p_{3/2}$ and Ti $2p_{1/2}$ in Mn-doped films are found at 459.2 and 464.9 eV, respectively (Fig. 4(b)). Again the peak separation is 5.7 eV indicative of the presence of Ti^{4+} (TiO_2) in the film. However, these energy peaks corresponding to Ti $2p_{3/2}$ and Ti $2p_{1/2}$ have a positive shift of ~0.8 eV as compared to pure TiO_2 film. This indicates positively charged surface of doped TiO_2, which is due to the presence of dopant metal ions. Similar results have also been observed by Jiang and Gao [2].

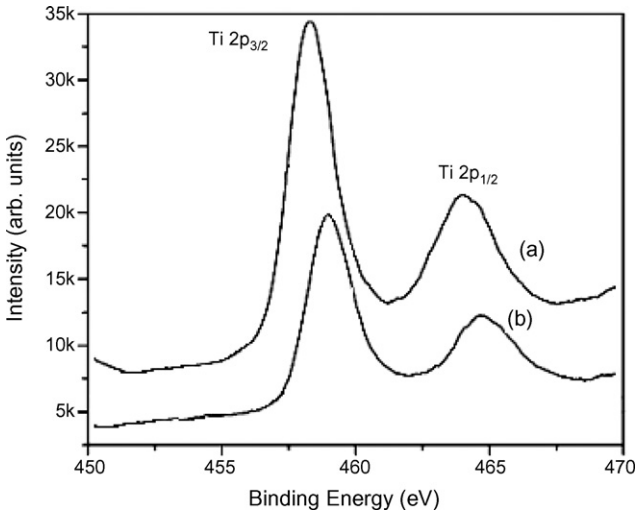

Fig. 4. X-ray photoelectron spectroscopy Ti 2p core level of (a) pure and (b) 5 mol% Mn-doped TiO_2 film.

Fig. 5 shows XPS of O 1s core level in the pure and Mn-doped TiO_2 films. The core level O 1s peak is observed at 529.7 eV for pure TiO_2, while in case of Mn-doped films, the core level O 1s is broadened as compared to undoped one. More OH^- groups are expected on the surface of Mn-doped film, the XPS peak corresponding to hydroxyl groups has reported to exist very close

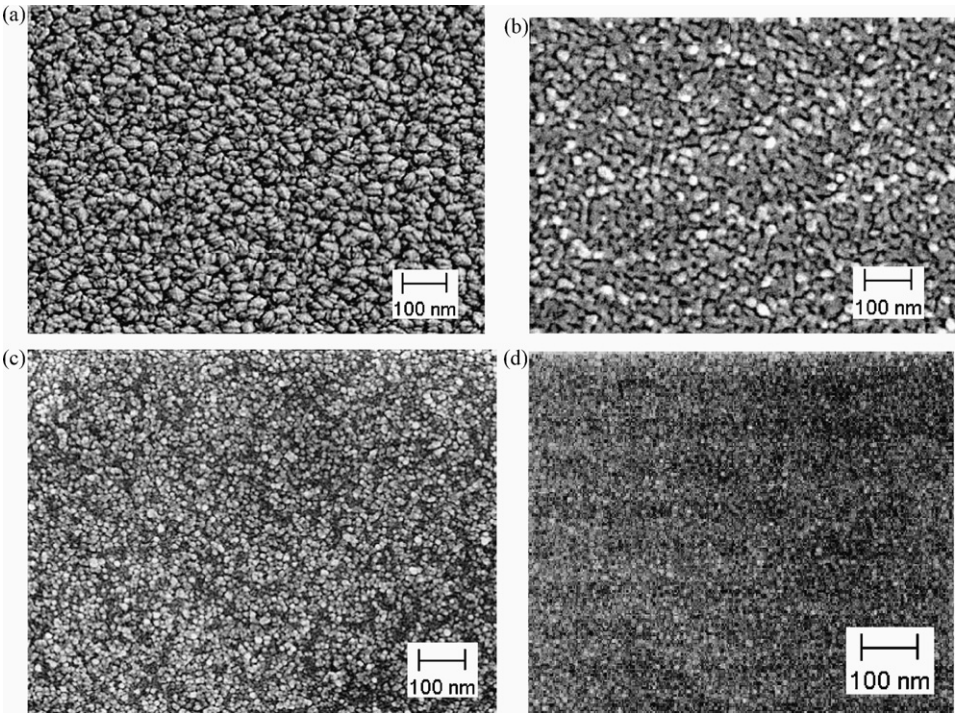

Fig. 3. SEM spectra of (a) pure TiO_2 film, (b) 2 mol%, (c) 5 mol% and (d) 8 mol% manganese doped TiO_2 film on soda glass annealed at 450 °C for 1 h.

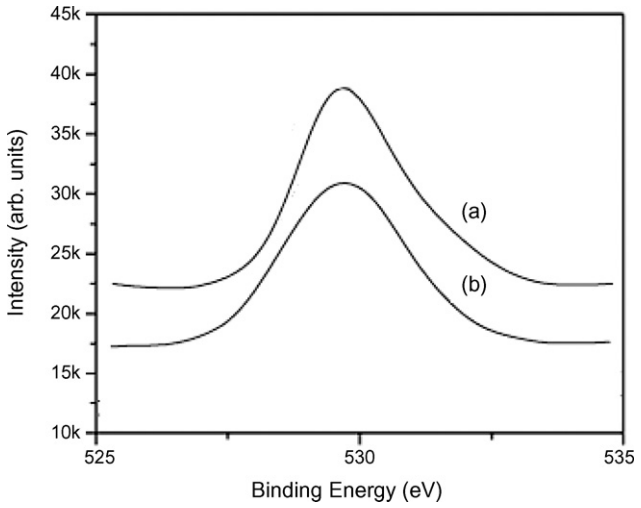

Fig. 5. X-ray photoelectron spectroscopy O 1s core level of (a) pure and (b) 5 mol% Mn-doped TiO_2 film.

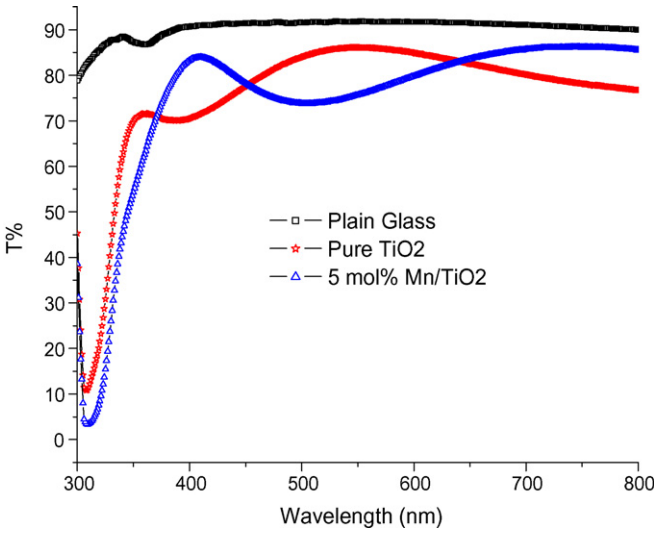

Fig. 7. Transmittance spectra of pure and manganese doped TiO_2 films.

to the O 1s peak (1.2 eV) [20]. The peaks due to both these sources merges and results in broader single peak.

XPS of Mn 2p core level of the Mn-doped TiO_2 film is shown in Fig. 6. The core level of Mn 2p3/2 and 2p1/2 shows binding energy peaks at 641.7 and 653.3 eV, respectively. These peaks with energy separation of 11.4 eV can be assigned to Mn^{2+} ions [19], which indicates that Mn exists in bivalent state, lower than Ti in these samples.

3.3. Optical studies

The transmittance of uncoated glass is about 91% over the visible light spectral region and its absorption edge is around 330 nm. The transmission spectra of TiO_2 and Mn/TiO_2 films on glass substrates show some different features (Fig. 7). For pure TiO_2 films, transmittance is ~76% at longer wavelength (~800 nm) and gradually rises at short wavelengths until it reaches its first maximum value of 85% at around 550 nm. After that, the transmittance decreases and rises again, and at about 380 nm it decreases rather quickly, finally approaches zero around 330 nm. The fast decrease below 380 nm is due to absorption of light caused by the excitation of electrons from the valence band to the conduction band of TiO_2. The oscillation of the curve between 800 and 380 nm is due to the interference associated with reflection from TiO_2 film surface and the substrate-film interface reflection. The band gap absorption in Mn-doped samples begins at slightly longer wavelengths w.r.t. undoped samples. Two distinct slopes have been observed in the band edge absorption of doped samples, which clearly indicates the presence of additional energy levels in the forbidden gap in case of doped samples. We have calculated the magnitude of these energies with the help of Tauc relation [21] $\alpha h\nu = A(h\nu - E_g)^m$ from the plot $(\alpha h\nu)$ versus photon energy $h\nu$ by taking $m = 2$ for indirect transitions (Fig. 8), where $\alpha = (1/d)\ln(1/T)$; d and T being thickness and transmittance, respectively. This plot gives two absorption energies viz, 3.45 and 2.82 eV for doped samples. The higher value of absorption energy i.e. 3.45 eV, matches to the value in undoped sample, hence it is assigned to the conduction band edge. The other lower energy value has been attributed to the strong absorption due localized levels existing in the forbidden gap because of Mn doping.

Photoluminescence spectra of undoped and doped TiO_2 films are shown in Fig. 9. Photoluminescence (PL) peak having FWHM

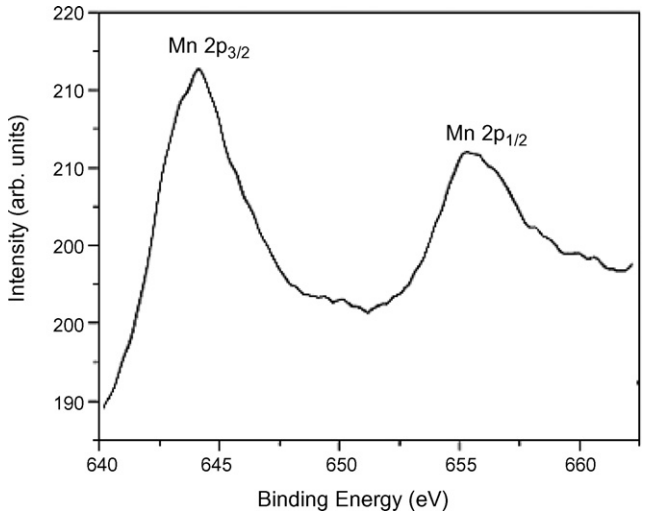

Fig. 6. X-ray photoelectron spectroscopy Mn 2p core level of 5 mol% Mn-doped TiO_2 film.

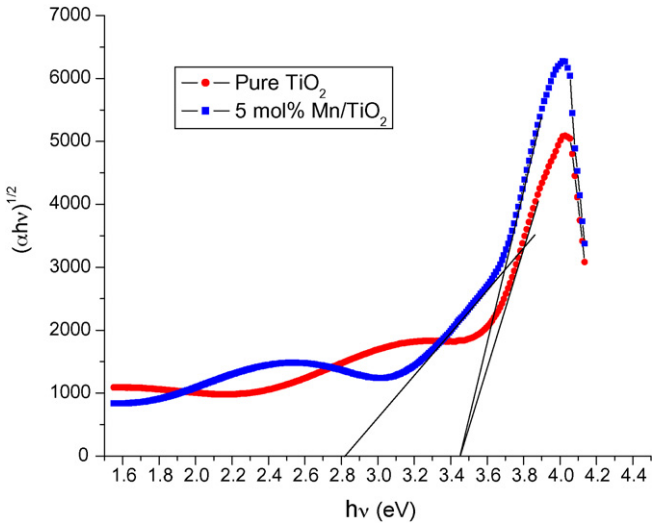

Fig. 8. Plot of $(\alpha h\nu)^{1/2}$ vs. $h\nu$.

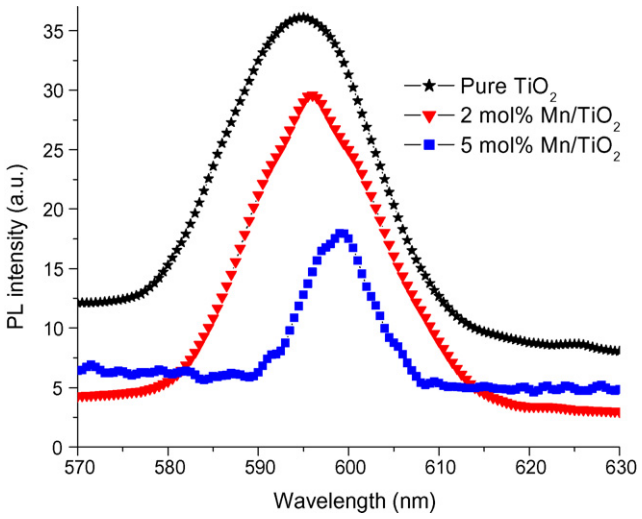

Fig. 9. Photoluminescence spectra of pure and Mn-doped TiO_2 films.

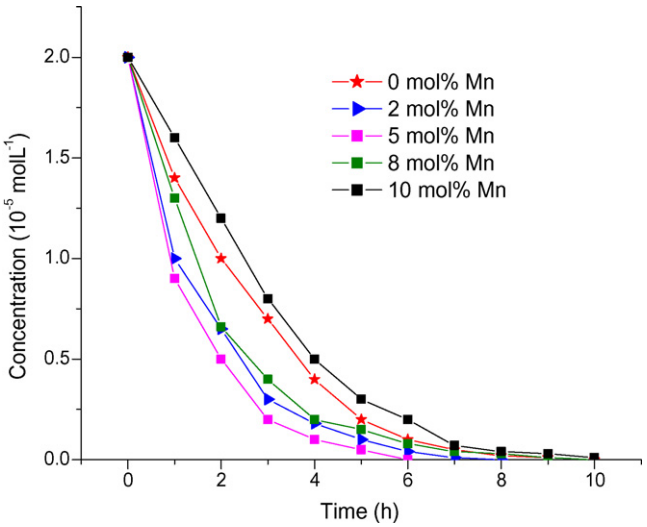

Fig. 11. The photodegradation rate of methylene blue solution with Mn-doped TiO_2 films under UV light.

~0.08 eV positioned at ~595 nm (2.08 eV) resembles in shape with the luminescence spectrum of other titanates containing TiO_6 octahedra. Stokes shifted emission band by ~1.2 eV results from the fundamental charge transfer transitions between Ti^{4+} and O^{2-}, localized on the octahedron. In such a process the energy of excited state is lowered by transferring from one site to the neighboring site forming an exciton band, the width of which depends upon the co-ordination number of TiO_6 octahedra. Such excitons exist in self trapped state which are characterized by strong electron phonon coupling and small exciton bandwidth. Narrow PL emission band is due to the fact that exciton band involving Ti 3d level is usually narrow. The exciton bandwidth of anatase TiO_2 is even narrower than the rutile phase because of; (i) lower co-ordination number, (ii) larger unit cell with smaller brillouin zone which contributes to the narrowing of bands which in turn favors localization. Photoluminescent intensity decreases by Mn doping, while the peak position is unaltered. Quenching of photoluminescence intensity suggests that there is transfer of photoexcited electrons to Mn on crystallite surface which reduces the exciton concentration and in turn the photoluminescent intensity. The transfer of electrons to the Mn atoms results in increased life time of the photogenerated charge carriers; this is confirmed by enhanced photocatalytic activity of the doped sample. The non-radiative recombination processes suggested by Rahman et al. [22] in Pb doped samples does not appear to be the reason for quenching of photoluminescent intensity in these samples.

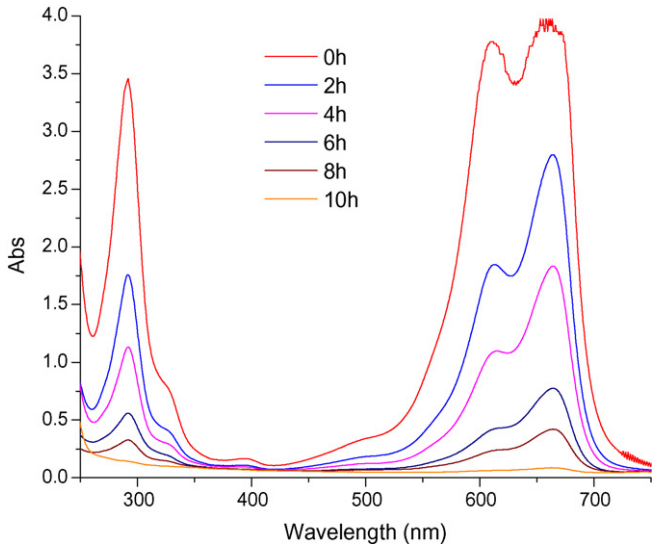

Fig. 10. Variation in UV–vis absorption spectra of aqueous methylene blue solution of pH 6–7 treated with TiO_2 film under UV light.

3.4. Photocatalytic studies

Typical absorption spectra of methylene blue (MB) solution, initial concentration 2×10^{-5} mol/l, in which pure TiO_2 film was settled and exposed to UV radiations for different time durations up to 10 h, is shown in Fig. 10. These studies are performed on undoped and Mn-doped TiO_2 films up to 10 mol% Mn concentration. Intensity of the absorption peak at 660 nm is plotted versus exposure time (Fig. 11). It is evident from this figure the degradation rate of MB increases with increase in Mn content in the film up to 5 mol% further increase in the Mn concentration leads to anomalous behavior.

Detailed studies of Houas et al. [23] have shown that methylene blue degrades in to colourless final products, CO_2, SO_4^{2-}, NH_4^+ and NO_3^-, by titanium based photocatalysis. Further the titanium based photocatalytic oxidation in water is not selective as compared to selective oxidation in pure organic gaseous or liquid phase of aliphatic or substituted aromatic hydrocarbons performed with the same titania catalyst. There are two oxidative agents in TiO_2: (i) photogenerated holes h^+ in the valence band, which are mainly responsible for photo-kolbe reaction and (ii) the $OH^\bullet$ radicals, which are strongly active and degrading but non-selective agents. $OH^\bullet$ radicals can be produced either by oxidation of water by holes or transient formation of hydrogen peroxide radicals.

$$(H_2O \Leftrightarrow H^+ + OH^-) + h^+ \rightarrow H^+ + {}^\bullet OH$$

– *oxidationofwaterbyholes*

$$\left.\begin{aligned} &O_2(g) + e^- \rightarrow {}^\bullet O_2^- \\ &O_2^{\bullet -} + H^+ \rightarrow HO_2^\bullet \\ &2HO_2^\bullet \rightarrow H_2O_2 + O_2 \\ &H_2O_2 + e^- \rightarrow OH^- + {}^\bullet OH \end{aligned}\right\} \text{transient formation of hydrogen peroxide}$$

In the degradation of methylene blue, $OH^\bullet$ radicals are supposed to attack the $C-S^+=C$ functional group, which is in direct coulombic interaction with titania surface. Therefore, first

step is the cleavage of C – S^+ = C functional group bonds, which induces the opening of the central aromatic ring containing both heteroatoms, S and N. second and third attacks by the •OH radical lead to dissociation of two benzene rings and finally the formation of sulphonic acid (R–C_6H_4–SO_3H). Now the sulphur has reached its final stable and maximum oxidation degree of +6. Fourth attack by •OH radical leads to release of SO^{4-} ions and R–C_6H_4• radical, which can further react with either •OH giving phenolic compound or with •H radical. Similar attacks at the N=C site leads to the formation of NH_4^+ or NO_3^- ions and photo-kolbe process is responsible for generation of CO_2.

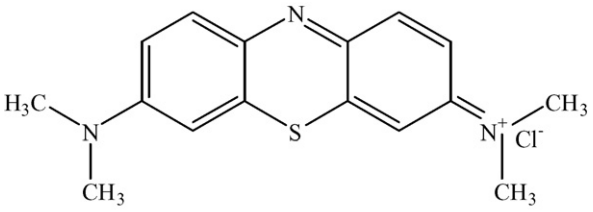

Methylene Blue

To enhance the degradation rate or photocatalytic activity in the sample, it is necessary that more charge carriers (electrons and holes) should be available for the above reactions. Availability of charge carriers under solar exposure conditions can be increased by either shifting the absorption edge to longer wavelength side, so as more charge carriers are generated and/or by increasing the life time of the photogenerated charge carriers, so that they can undergo the desired reaction before being destroyed by radiative recombination. Optical studies (Fig. 8) indicate introduction of additional energy level, in Mn-doped samples, at 2.82 eV above the valence band edge in the forbidden gap. But does this helps in enhancing the photocatalytic activity of the sample? As the level due to doping is ~0.63 eV below the conduction band edge, therefore thermal excitation of photoelectrons from dopant level to conduction band edge is not possible ($k_B T_{300\ K} \sim 0.030$ eV). Two photon absorption processes, similar to dye sensitization, is a matter of investigation, but such processes are generally prone to low quantum yield due to the narrowness of this band.

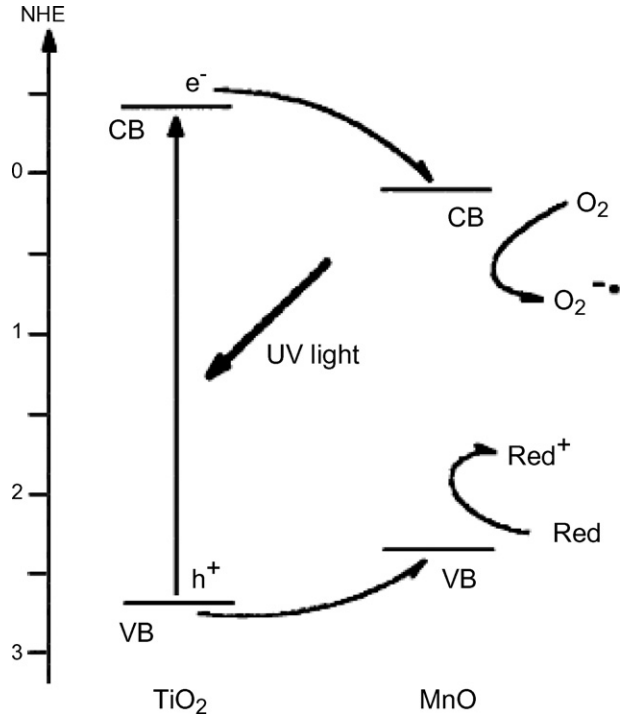

Fig. 12. Schematic representation of photocatalytic mechanism on Mn/TiO_2 surface under UV irradiation.

Another process is separation of charge carriers due to scavenging of photogenerated electrons by dopant ions. This process increases the life time of charge carriers, so that they can take part in photocatalytic processes. Band positions (conduction and valence) of MnO relative to TiO_2 are such that thermodynamic considerations support this phenomenon for, both electrons as well as holes. But due to large difference, about two orders, in mobilities of electrons and holes, transition of electrons from TiO_2 to MnO is considered. Also the photogenerated electrons preferentially go to Mn rather than oxygen as the transfer time to oxygen is reported to be of the order of milliseconds [17]. The electrons accumulated on the particle make the surface negatively charged, which helps in adsorption of dye molecules (MB dye is basic in nature) on the particle and helps to increase the photodegradation rate. Photocatalytic processes on Mn-doped TiO_2 surfaces are depicted schematically in Fig. 12.

Photodegradation on Mn-doped TiO_2 surface can be represented by the following equations.

Charge pair generation under UV irradiation

$$TiO_2 + h\nu \rightarrow h_{vb}^{+} + e_{cb}^{-}$$

$$Ti^{4+} + e_{cb}^{-} \rightarrow Ti^{3+}$$

$$O^{2-} + h^{+} \rightarrow O^{-}$$

Charge pair trap in presence of Mn^{2+} ion

$$Mn^{2+} + Ti^{3+} \rightarrow Mn^{+} + Ti^{4+} \quad \text{electrontrap}$$

$$Mn^{2+} + O^{-} \rightarrow Mn^{3+} + O^{2-} \quad \text{holetrap}$$

According to the crystal field theory, Mn^{3+} and Mn^{+} ions are relatively unstable as compared to Mn^{2+} ions, which have half-filled d orbital (d^5). Therefore, there is tendency for the transfer for the trapped charges from Mn^{3+} and Mn^{+} to the interface to initiate the following reactions [14].

$$Mn^{+} + O_2 \rightarrow Mn^{2+} + O_2^{-} \quad \text{electronrelease}$$

$$Mn^{3+} + OH^{-} \rightarrow Mn^{2+} + {}^{\bullet}OH \quad \text{holerelease}$$

Thus photogenerated superoxide ion ($O_2^{\bullet -}$) and hydroxyl radical (•OH) are highly reactive and degrade the methylene blue. Photodegradation profiles of MB by Mn-doped films under UV irradiation are shown in Fig. 11. Degradation rate has been observed to increase with increase in Mn concentration up to 5 mol% after which there is a decrease in the degradation rate. The observed profiles can be fitted in to the following exponential relationship.

$$C = C_0 \exp^{(-kt)}$$

where C_0 is the initial concentration of dye, C the concentration after exposure interval t and k is thereaction rate constant. The plot of the log concentration of dye versus time of irradiation yielded a straight line; the slope of this line is the rate constant k. The calculated rate constants for different Mn concentrations are listed in Table 1. In general the photocatalytic reaction follows the Langmuir-Hinshelwood mechanism. For dilute solutions the reaction is apparently first order.

The increase in photocatalytic activity due to Mn doping is attributed to three reasons (i) increase in life time of photogenerated electrons and holes due to scavenging of electrons by Mn, (ii) charging the particle surface due to electron on the surface, which enhances the adsorption of dye molecules, and (iii) decreased crystallite size, as evident from XRD studies, increases

Table 1
Experimental values of rate constant of undoped and Mn-doped TiO_2 films for degradation of methylene blue under UV and visible light exposure conditions

Concentration of manganese in TiO_2 film (mol%)	Rate constant (k) under UV light exposure (h^{-1})	Rate constant (k) under vis light exposure (h^{-1})
0	0.27	0.052
2	0.31	0.051
5	0.36	0.092
8	0.25	0.049
10	0.24	0.043

the exposed surface area to incoming radiations thereby enhancing the quantum yield for photon absorption. But increased dopant concentration also adds to the defects in the crystallite, these defects hinders the crystallization of the material. Carp et al. and Anpo-Tshima et al. [24,25] have shown that photoactivity is the property of crystalline anatase TiO_2, amorphous TiO_2 is found to be non-photoactive. Therefore, at increased dopant concentration the amorphicity of the film increases due to which less photoactivity, even less than undoped TiO_2, is observed in films having 10 mol% Mn concentration.

To examine the role of dopant band in forbidden gap of pure TiO_2, we have studied the photocatalytic activity (degradation of MB) under visible exposure only with commercial electric bulb (100 W). The residual dye concentration after different exposure intervals is shown in Fig. 13. We have observed very small degradation rate for MB (~1/6th to that under UV exposure), under these conditions. This suggests a very weak absorption of photon, which leads to creation of charge carriers, via this band also excitation of dye molecule can be ruled out. Therefore, the main role of dopant is to take the photoelectrons, thereby increasing the life time of photogenerated carriers.

3.5. Photo-induced hydrophillicity

Changes in the water contact angle on Mn-doped TiO_2 films, induced by 0.5 mW cm^{-2} UV light irradiation for 25 min are shown in Fig. 14. The contact angle of the sample which consists of pure TiO_2 is about 18°. It reduces with increasing dopant concentration and approaches 0° for 5 mol% Mn concentration. After putting the samples for 24 h in a dark place, the contact angle goes up from 18°

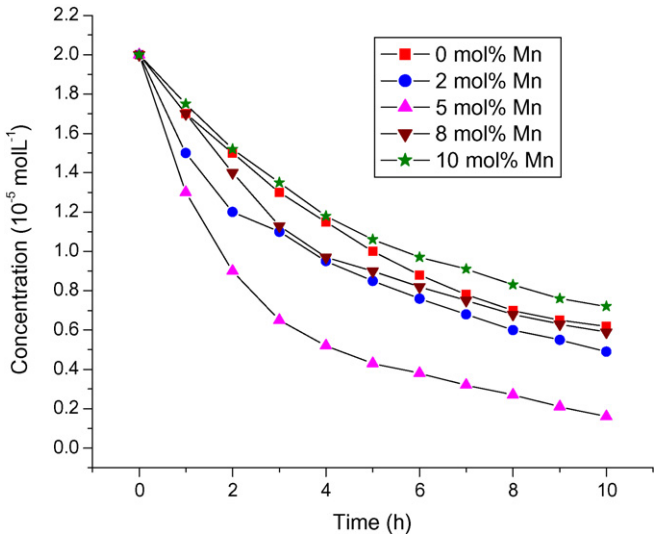

Fig. 13. The photodegradation rate of methylene blue solution with Mn-doped TiO_2 films under visible light.

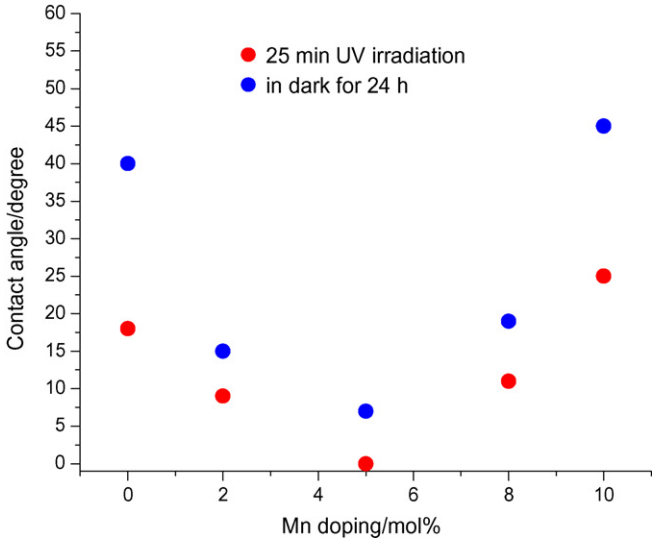

Fig. 14. Dependence of the photo-induced change in the water contact angle of Mn/TiO_2 films.

to 40° with the pure TiO_2 film and from 0° to 7° with 5 mol% Mn-doped TiO_2 film. The results showed that with 5 mol% Mn/TiO_2 film, the contact angle of the film increases very slowly and can maintain the super-hydrophilic state for a long time in the dark.

The phenomenon of hydrophillicity is well understood for pure TiO_2 [26,27]. The mechanism of hydrophillicity is different from photocatalytic activity, the electrons and holes are still produced but they react differently. The electrons tend to reduce the Ti(IV) cations to Ti(III) state, the holes oxidize O_2^- anions. In this process oxygen atoms are ejected, creating oxygen vacancies. Water molecules can than occupy oxygen vacancies, producing adsorbed OH groups, which tend to make the surface hydrophilic. In spite of the different mechanisms of photocatalytic effect and hydrophilic effect, the correlation between the two is obvious. The photo-induced hydrophillicity of the film is closely related to the photocatalytic removal of organic substances from the film surface. The synergetic effect of photocatalysis and hydrophillicity can be understood as; because more OH groups can be adsorbed on the surface due to hydrophillicity, the photocatalytic activity is enhanced. So hydrophillicity can improve photocatalysis. On the other hand film surface can adsorb contaminated compounds which tend to convert the hydrophilic surface to the hydrophobic one. Photocatalysis can decompose the organic dirt on the film surface resulting in the restoration of hydrophillicity. This shows that photocatalysis can improve hydrophillicity and maintain this characteristic for long time. Mn is supposed to enhance the hydrophillicity by taking an electron from Ti^{4+} to render it in Ti^{3+} state, while holes remaining at the valence band of TiO_2 (conduction band edge of Mn is at lower level in comparison to conduction band edge of TiO_2) thereby initiating the process for oxygen removal and hence hydrophillicity of the film.

4. Conclusions

Manganese doped TiO_2 film derived by sol–gel process are more photoactive than undoped one. The reason of enhancement in photoactivity is due to three factors: (i) increase in life time of photogenerated charge carriers, (ii) more adsorption of organic molecules, to be degraded, due to charged crystallite surface and (iii) increased surface area due to small crystallite size. The crystallinity of TiO_2 decreases with increase in dopant concentration, due to which photoactivity increases only up to certain dopant concentration only. At higher dopant concentration

increased amorphicity is supposed to kill the photoactivity. Photoluminescence emission is Stoke's shifted by ~1.2 eV due to the formation of self trapped exciton band by charge transfer between Ti^{4+} and O^{2-} on TiO_6 octahedra. Quenching of photoluminescence by Mn doping takes place due scavenging of photogenerated electrons by Mn. Charging of film surface by Mn doping shifts Ti p lines by ~0.08 eV.

Mn doping generates an additional level at ~2.82 eV above the valence band. This band may have very small effect on photoactivity of Mn-doped TiO_2 films by exciting electrons across the band gap by two photon process from visible range.

Hydrophillicity and photoactivity arise due to two different mechanisms, but they go side by side i.e. if one increases the other also increases or vice versa, this is due to interfacial nature of the two processes. Photocatalytic reaction follows the Langmuir-Hinshelwood mechanism for dilute solutions and the reaction is apparently first order.

Acknowledgements

Authors are highly thankful to Director, National Physical Laboratory, New Delhi, India for providing laboratory facilities to carryout this research and one of the authors, Dr. Sunil Dutta Sharma, in thankful to Council of Scientific and Industrial Research (CSIR), New Delhi, India for financial assistance.

References

[1] H. Chao, Y. Yun, H. Xingfang, A. Larbot, Appl. Surf. Sci. 200 (2002) 239.
[2] H. Jiang, L. Gao, Mater. Chem. Phys. 77 (2002) 878.
[3] W. Zhang, Y. Li, S. Zhu, F. Wang, Catal. Today 93–95 (2004) 589.
[4] I.H. Tseng, J.C.S. Wu, H.Y. Chou, J. Catal. 221 (2004) 432.
[5] E.D. Palik, Handbook of Optical Constant of Solids, vol. II, Academic Press, 1991, p. 795.
[6] S.J. Tsai, S. Cheng, Catal. Today 33 (1997) 227.
[7] H.P. Maruska, A.K. Ghosh, Sol. Energy 20 (1978) 443.
[8] C. Guillard, B. Beaugiraud, C. Dutriez, J.M. Hermann, H. Jaffrezic, N. Jaffrezic, M. Lacroix, Appl. Catal. B: Environ. 39 (2002) 331.
[9] J. Yu, X. Zhao, Q. Zhao, Thin Solid Films 379 (2000) 7.
[10] D. Dvoranova, V. Brezova, M. Mazur, M.A. Malati, Appl. Catal. B: Environ. 37 (2002) 91.
[11] M. Zhao, J. Yu, B. Cheng, H. Yu, Mater. Chem. Phys. 93 (2005) 159.
[12] L. Palmisano, V. Augugliaro, A. Sclajani, M. Schiavello, J. Phys. Chem. 92 (1988) 6710.
[13] E.B. Gracien, J. Shen, X. Sun, D. Liu, M. Li, S. Yao, J. Sun, Thin Solid Films 515 (2007) 5287.
[14] C.Y. Wang, C. Bottcher, D.W. Bahnemann, J.K. Dohrmann, J. Mater. Chem. 13 (2003) 2322.
[15] S. Karvinen, Solid State Sci. 5 (2003) 811.
[16] K. Okada, N. Yamamoto, Y. Kameshima, A. Yasumori, K. Mackenzie, J. Am. Ceram. Soc. 84 (2001) 1591.
[17] F. Chen, Y. Xie, J. Zhao, G. Lu, Chemosphere 44 (2001) 1159.
[18] Y. Ma, X.T. Zhang, Z.S. Guan, Y.A. Cao, J.N. Yao, J. Mater. Res. 16 (2001) 2928.
[19] J.F. Moulder, W.F. Stickle, P.E. Sobol, K.D. Bomben, Handbook of X-ray Photoelectron Spectroscopy, PerkinElmer, Eden Praitie, MN, 1992.
[20] B. Erdem, R.A. Hunsicker, G.W. Simmons, E.D. Sudol, V.L. Dimonie, M.S. El-Aasser, Langmuir 17 (2001) 2664.
[21] P.M. Kumar, S. Badrinarayanan, M. Sastry, Thin Solid Films 358 (2000) 122.
[22] M.M. Rahman, K.M. Krishna, T. Soga, T. Jimbo, M. Umeno, J. Phys. Chem. Solids 60 (1999) 201.
[23] A. Houas, H. Laccheb, M. Ksibi, E. Elaloui, C. Guillard, J.M. Herrmann, Appl. Catal. B: Environ. 31 (2001) 145.
[24] O. Carp, C.L. Huisman, A. Reller, Prog. Solid State Chem. 32 (2004) 33.
[25] M. Anpo-Tshima, S. Kodama, Y. Kobukawa, J. Phys. Chem. 91 (1987) 4305.
[26] R. Wang, N. Sakai, A. Fujishima, T. Watanabe, K. Hashimoto, J. Phys. Chem. B 103 (1999) 2188.
[27] M. Miyauchi, A. Nakajima, K. Hashimoto, T. Watanabe, Adv. Mater. 12 (2000) 1923.